Programmed Cell Death-Involved Aluminum Toxicity in Yeast Alleviated by Antiapoptotic Members with Decreased Calcium Signals[1]

Ke Zheng, Jian-Wei Pan, Lan Ye, Yu Fu, Hua-Zheng Peng[2], Bai-Yu Wan, Qing Gu[3], Hong-Wu Bian, Ning Han, Jun-Hui Wang, Bo Kang, Jun-Hang Pan, Hong-Hong Shao, Wen-Zhe Wang, and Mu-Yuan Zhu*

State Key Lab of Plant Physiology and Biochemistry, College of Life Sciences, Zhejiang University, Hangzhou 310058, China

The molecular mechanisms of aluminum (Al) toxicity and tolerance in plants have been the focus of ongoing research in the area of stress phytophysiology. Recent studies have described Al-induced apoptosis-like cell death in plant and animal cells. In this study, we show that yeast (*Saccharomyces cerevisiae*) exposed to low effective concentrations of Al for short times undergoes enhanced cell division in a manner that is dose and cell density dependent. At higher concentrations of Al or longer exposure times, Al induces cell death and growth inhibition. Several apoptotic features appear during Al treatment, including cell shrinkage, vacuolation, chromatin marginalization, nuclear fragmentation, DNA degradation, and DNA strand breaks, as well as concomitant cell aggregation. Yeast strains expressing Ced-9, Bcl-2, and PpBI-1 (a plant Bax inhibitor-1 isolated from *Phyllostachys praecox*), respectively, display more resistance to Al toxicity compared with control cells. Data from flow cytometric studies show these three antiapoptotic members do not affect reactive oxygen species levels, but decrease calcium ion (Ca^{2+}) signals in response to Al stress, although both intracellular reactive oxygen species and Ca^{2+} levels were increased. The data presented suggest that manipulation of the negative regulation process of programmed cell death may provide a novel mechanism for conferring Al tolerance.

Programmed cell death (PCD) comprises a series of genetically controlled events and plays important roles in various biological processes, from development to stress responses. Apoptosis, a highly regulated PCD, is morphologically and biochemically defined with some typical characteristics (Lawen, 2003). Although the precise mechanisms of PCD in many aspects are still far from clear, PCD is often mediated by two important molecular signals, reactive oxygen species (ROS) and calcium ions (Ca^{2+}; Brookes et al., 2004).

Bcl-2 family members can regulate PCD negatively (e.g. Bcl-2, Ced-9, and Bcl-XL) and positively (e.g. Bax and Bak). Bcl-2 and Ced-9 represent two of the most important antiapoptotic members in mammals and nematodes, respectively. Bcl-2 prevents many forms of PCD in a variety of cell types. The heterogeneous function of Bcl-2 family members in regulating cell death is conserved in plants (Mitsuhara et al., 1999; Dickman et al., 2001; Xu et al., 2004), suggesting that the PCD machinery of eukaryotic species may share some common elements. However, in spite of the detection of a Bcl-2-like protein by immunoblots (Dion et al., 1997), so far no homolog of Bcl-2 family members has been identified in plants and lower eukaryotes, suggesting that other PCD regulators may be employed in those species. Bax inhibitor-1 (BI-1), as one of the few endogenous cell death inhibitors in plants, is potentially a core regulator of PCD (Hückelhoven, 2004). BI-1 is dispensable for normal plant development, but plays a protective role against both biotic (e.g. fungal pathogen and fungal toxin) and abiotic (e.g. oxidative stress and heat shock) stresses (Chae et al., 2003; Matsumura et al., 2003; Eichmann et al., 2004; Kawai-Yamada et al., 2004; Watanabe and Lam, 2006). Interestingly, BI-1 is mainly located in the endoplasmic reticulum and associated perinuclear region, probably serving as a pore or ion channel downstream of oxidative stress (Xu and Reed, 1998; Kawai-Yamada et al., 2001; Chae et al., 2004; Kawai-Yamada et al., 2004).

Aluminum (Al) toxicity is a serious agricultural problem in the acid soil. The molecular mechanisms of Al toxicity and tolerance in plants have been the focus of ongoing research in the area of stress phytophysiology, and several possible mechanisms have been proposed to explain the action of Al toxicity. Due

[1] This work was supported by the National Natural Science Foundation of China (grant no. 30370876 to M.-Y.Z.; grant no. 30100115 to J.-W.P.) and the Provincial Natural Science Foundation of Zhejiang Province (grant no. G20050170 to M.-Y.Z.; grant nos. Z304414 and Y305317 to H.-Z.P.).

[2] Present address: Zhejiang Forestry Academy, Hangzhou 310023, China.

[3] Present address: Department of Biotechnology, Hangzhou University of Commerce, Hangzhou 310012, China.

* Corresponding author; e-mail myzhu@zju.edu.cn; fax 86–571–88206535.

The author responsible for distribution of materials integral to the findings presented in this article in accordance with the policy described in the Instructions for Authors (www.plantphysiol.org) is: Mu-Yuan Zhu (myzhu@zju.edu.cn).

www.plantphysiol.org/cgi/doi/10.1104/pp.106.082495

to the special chemical nature of Al, however, the mechanisms of Al toxicity remain largely obscure and controversial (Matsumoto, 2000; Kochian et al., 2004). Al toxicity in plants was associated with oxidative damage (Ezaki et al., 2000; Yamamoto et al., 2002; Devi et al., 2003; Pan et al., 2004) and blockage of Ca^{2+} channels (Huang et al., 1996; Kawano et al., 2004). Mechanisms of Al tolerance have been broadly classified as external exclusion and internal detoxification, and great efforts have been made to obtain Al-tolerant plants using biotechnological means (Ezaki et al., 2001; Delhaize et al., 2004; Sasaki et al., 2004). Most impressively, *ALMT1* was demonstrated as a major Al-tolerant gene conferring effective protection to crop species (Delhaize et al., 2004). In humans, Al is considered to be a neurotoxic metal and often connected with the onset of neurodegenerative disorders such as Alzheimer's disease (Savory et al., 2003). Recent studies have described some apoptotic hallmarks that appeared upon Al treatment in plant and animal cells, suggesting that Al can induce apoptosis-like cell death (Suárez-Fernández et al., 1999; Pan et al., 2001; Aremu and Meshitsuka, 2005).

Innumerable reports imply similar molecular mechanisms and biochemical features in the PCD of animals, plants, and yeast. Although yeast apoptosis is still controversial (LeBrasseur, 2004), abundant evidence suggests that yeast is an excellent model system because it has been extensively characterized both biologically and genetically (Fleury et al., 2002b; Jin and Reed, 2002; Madeo et al., 2004). Moreover, yeast has several advantages for research on Al toxicity and tolerance (MacDiarmid and Cardner, 1996), and parallels between yeast and plant systems are evident on some mechanisms of Al toxicity (Schott and Gardner, 1997; MacDiarmid and Gardner, 1998; Ezaki et al., 1999; Anoop et al., 2003). Therefore, clarifying how Al induces yeast cells to undergo PCD would be helpful to better understand the complex mechanisms of Al-induced PCD in plants. This study showed the effect of Al in yeast (*Saccharomyces cerevisiae*) mainly concerned with PCD and the potential roles of antiapoptotic members in Al tolerance, suggesting that manipulation of the negative regulation process of PCD may provide a novel mechanism for conferring Al tolerance.

RESULTS

Positive and Negative Effects of Al Toxicity on Cell Growth in Yeast

In yeast, as reported in plants and animals, the Al inhibitory effect on cell growth (OD_{600} values) was positively correlated with Al concentrations (Fig. 1A). In 2 mM Al treatment, however, cell density was higher than in any other level treatment within the first 10 h and then its predominance was decreased gradually, indicating that 2 mM Al might promote yeast growth in our present culture system. Further data showed that

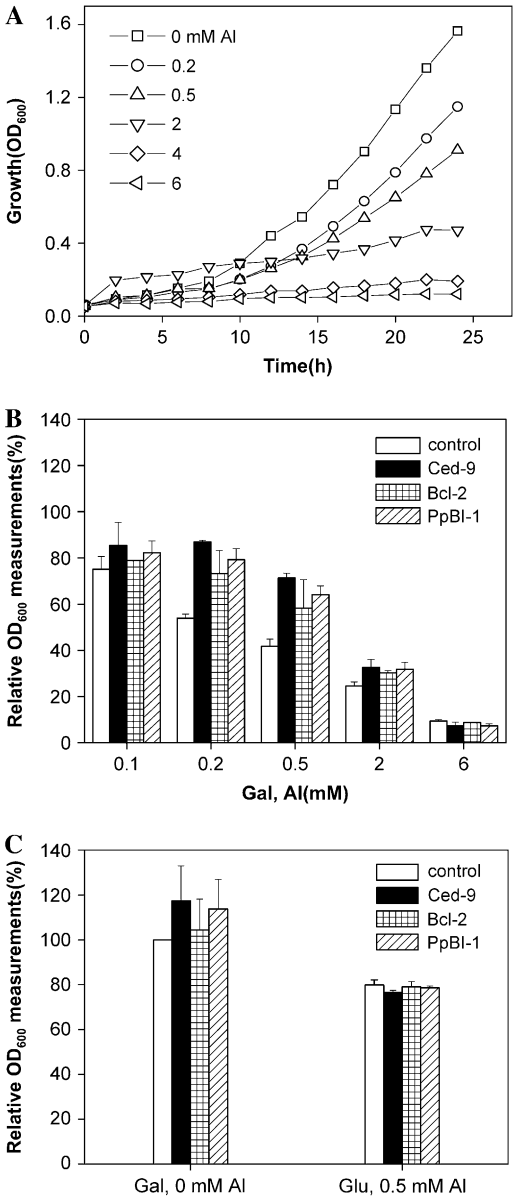

Figure 1. Yeast growth under Al treatment. A, Yeast strain EGY48 transformed with empty vector pGilda (control) was incubated in liquid SD/Gal-Raf/His medium (pH 4.0) containing a series of $AlCl_3$ levels. Cell densities (OD_{600} values) were determined at 2-h intervals over a 24-h period. It was shown that 2 mM Al promoted cell growth at the beginning of growth. B, Comparison of growth between yeast cells expressing Ced-9, Bcl-2, PpBI-1, and the control cells incubated in liquid SD/Gal-Raf/His medium (pH 4.0) added serous doses of $AlCl_3$ for 24 h. Relative OD_{600} measurements were calculated as the OD_{600} of treated cells divided by that of untreated cells. The value of strains with no Al treatment was set at 100%. C, Comparison of growth among yeast strains either incubated in SD/Gal-Raf/His medium (pH 4.0) without Al (left) or in SD/Glu/His medium (pH 4.0) with 0.5 mM Al (right). Relative OD_{600} measurements of the control cells (left) or those of strains without Al (right) were set at 100%.

Al significantly enhanced cell growth in a range of 1 to 4 mM Al levels and the cell density (OD_{600} values) at the 2 mM Al level reached a peak value of approximately 100% higher than that with no Al (Fig. 2A). Furthermore, at 2 mM Al, lower initial cell density could lead to a higher promotional effect for longer periods (Fig. 2B). To rule out the possibility that enhanced cell growth may result from a reduced pH value caused by Al or anions such as Cl^- and SO_4^{2-}, further tests were conducted. As shown in Figure 2C, with pH values lowered from 4.0 (the pH of medium without Al) to 3.3 (the altered pH when Al is added), Cl^- and SO_4^{2-} could not significantly enhance cell growth. To exclude another possibility that increased OD_{600} values caused by 2 mM Al treatment was due to increased cell size instead of accelerated cell division, we counted the cell number under a microscope. The data on cell number (Fig. 2D) are consistent with the results on cell density (Fig. 2C). Other data from flow cytometry showed that 2 mM Al induced more small cells than the control without Al (Fig. 2, E–G). These data suggested that enhanced cell division during the early stage of Al treatment resulted from Al itself.

Al-Induced PCD in Yeast

Some Al-induced PCD hallmarks have been reported in both plants (Yamaguchi et al., 1999; Pan et al., 2001; Boscolo et al., 2003) and animals (Suárez-Fernández et al., 1999; Aremu and Meshitsuka, 2005). In this study, we want to confirm whether there also exist some similar PCD characteristics during Al-caused cell death in yeast. Cell viability assays were performed by counting cell number and staining using propridium iodide (PI) alone or together with fluorescein diacetate (FDA). From our results, cell viability was negatively correlated with Al concentrations (except for the data of 54 mM Al treatment, repeated five

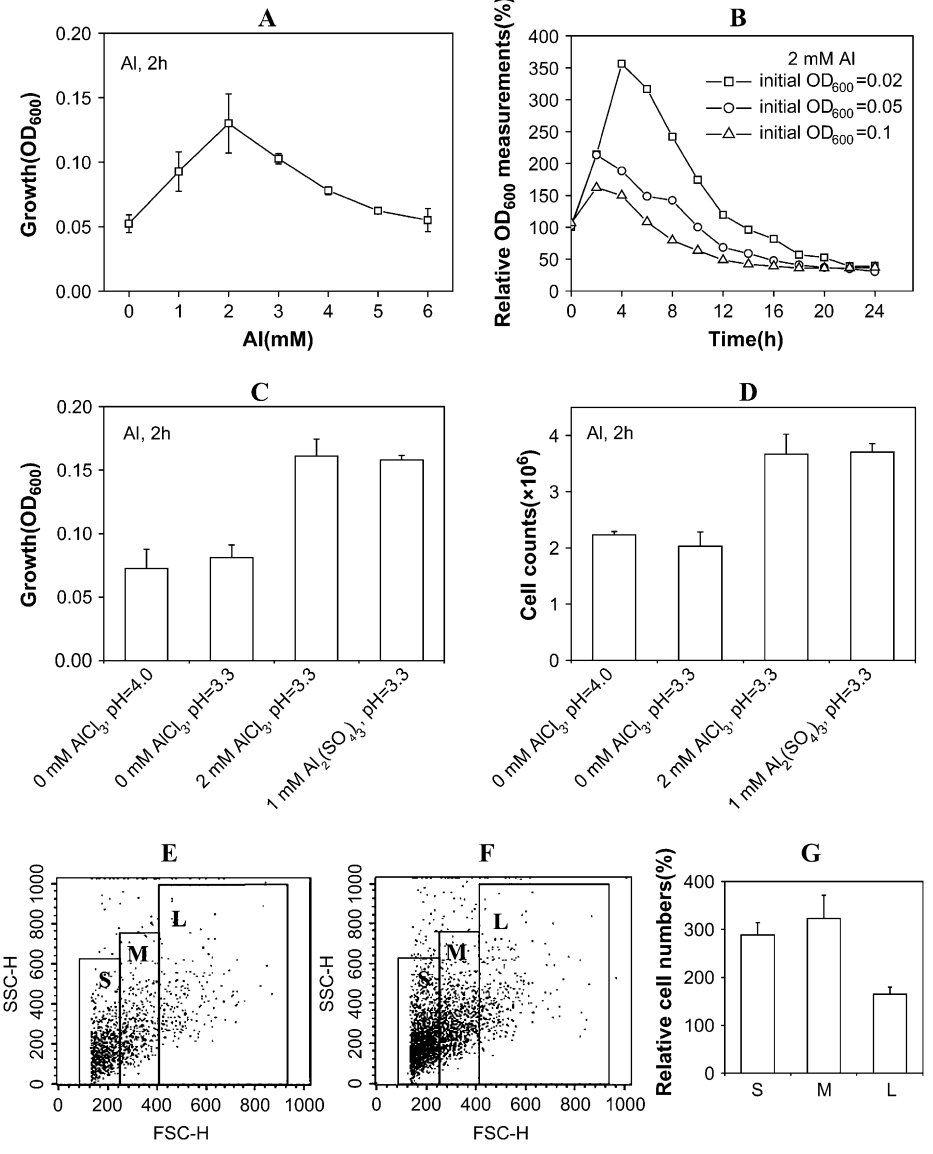

Figure 2. Effect of Al toxicity on cell division in yeast. A, OD_{600} measurements of the control cells incubated in SD/Gal-Raf/His medium upon indicated Al levels for 2 h. B, Growth of the control cells with different initial cell densities (OD_{600} = 0.02, 0.05, and 0.1, respectively) incubated in SD/Gal-Raf/His with 2 mM Al during 24 h. OD_{600} values were measured at 2-h intervals, and relative OD_{600} values were calculated as a percentage of corresponding controls. C and D, Comparison of cell growth presented with OD_{600} values (C) or cell numbers (D) between cells treated with 0 mM $AlCl_3$ (pH 4.0), 0 mM $AlCl_3$ (pH 3.3), 2 mM $AlCl_3$ (pH 3.3), and 1 mM $Al_2(SO_4)_3$ (pH 3.3) for 2 h. E and F, Cells were treated with no Al (E) or 2 mM Al (F) for 2 h, and then cell numbers with different sizes (S, small; M, middle; L, large) were cytometrically counted. G, Relative cell numbers in Al-treated cells (F) were expressed as a percentage of the untreated control (E). Initial OD_{600} is 0.05, except for B.

times) and treatment time (Fig. 3, A, C, E, and F), indicating that Al-caused cell death occurred basically in a time- and dose-dependent manner. Remarkably, abnormal aggregation of dead cells occurred at the 6 mM Al level (Fig. 3F).

We simultaneously examined some typical markers of apoptosis in yeast using scanning and transmission electron microscopy. To avoid the complicated influence of low-level Al-enhanced cell division on analysis of results, we mainly adopted 6 mM Al treatment, which directly inhibits yeast growth, to perform PCD-related assays. From our data herein, 6 mM Al induced typical apoptotic characteristics, including cell shrinkage (Fig. 4, A and B), nuclear fragmentation, vacuolation, and chromatin marginalization (Fig. 4, C–F). 4′,6-Diamidino-2-phenylindole (DAPI)-stained cells also exhibited Al-induced nuclear fragmentation and DNA degradation (Fig. 4, G and H). To provide direct evidence for DNA degradation in the process of Al-induced cell death, TUNEL assay was conducted using confocal laser-scanning microscopy. As shown in Figure 4, I to N, TUNEL positive signals could be detected in Al-treated yeast cells. Analysis of DNA content by flow cytometry showed a significantly increased percentage of apoptotic cells under Al stress compared with the control without Al (Fig. 4, O and P). These results fully demonstrated that Al-induced cell death is a process of PCD.

Heterogeneous Antiapoptotic Members Improve Yeast Growth and Viability under Al Stress

To further prove Al-induced PCD, we first isolated a novel BI-1 gene from *Phyllostachys praecox* (*PpBI-1*)

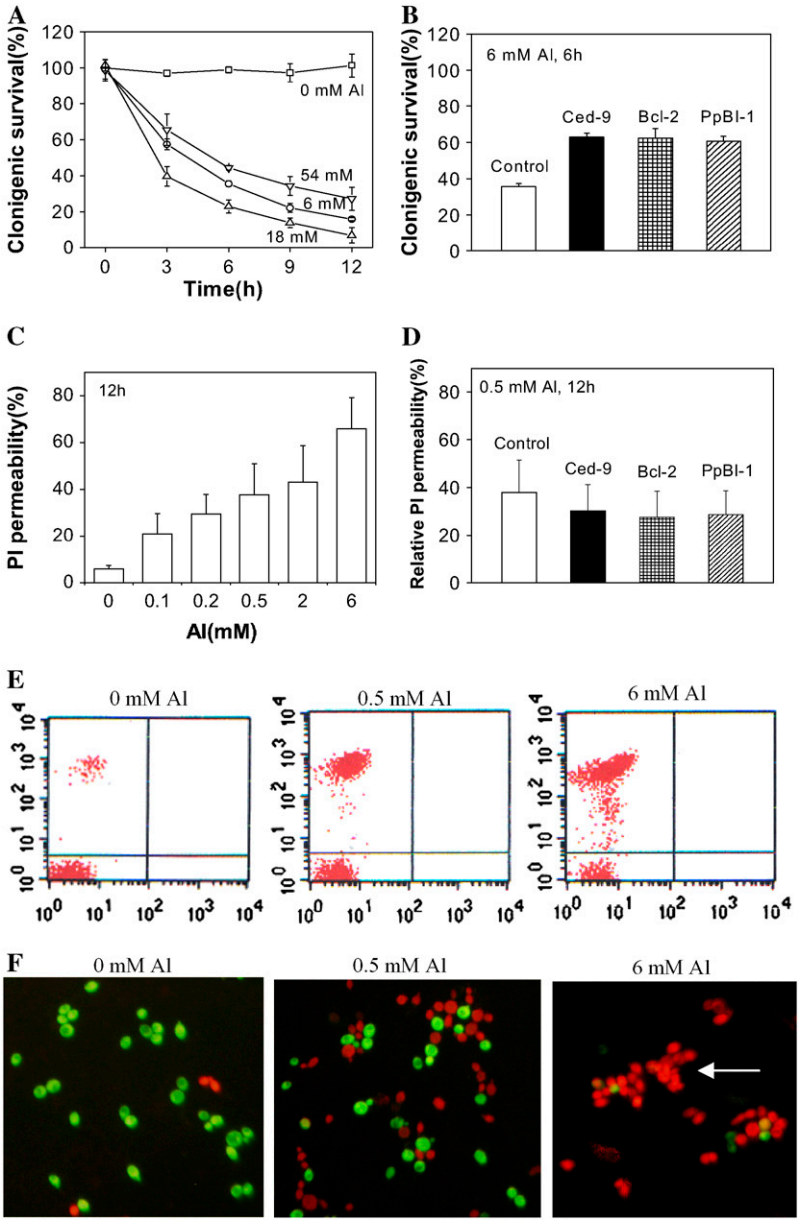

Figure 3. Viability assays of yeast cells under Al stress. A, Clonigenic survival rates of control cells treated with Al for 12 h. Values were calculated as a percentage of clonigenic numbers without Al treatment. Viability with no Al for 0 h was set at 100%. B, Clonigenic survival rates of cells transformed with antiapoptotic genes upon 6 mM Al stress for 6 h. Calculation method is the same as in A. C, Percent PI permeability of the control cells upon indicated Al levels for 12 h. Values were produced by dividing the PI-stained cell numbers by the total ones. D, Comparison of the relative PI permeability between the transgenic strains with the control. Values were calculated by the formulation 1 − (% of PI negative cells with Al/% of PI negative cells without Al). E, Distribution of PI positive and negative cells by flow cytometry. F, Cells stained by FDA-PI observed under a fluorescent microscope. Viable cells were green fluorescent and dead cells were red fluorescent. The arrow points to the aggregated cells under Al stress.

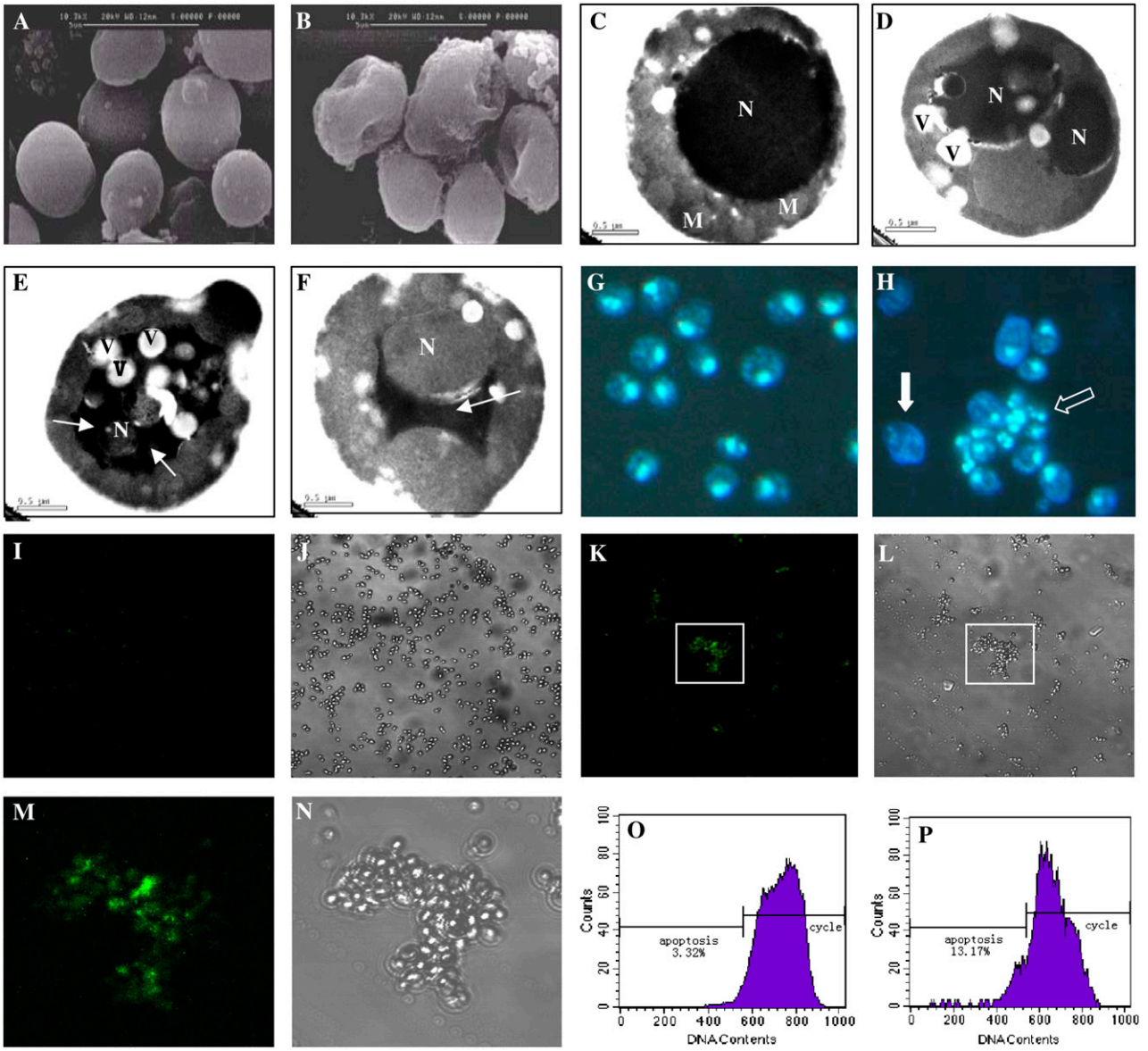

Figure 4. Characterization of Al-induced PCD in yeast. Yeast cells were treated with no Al (A, C, G, I, J, O) and 6 mM (B, D, E, F, H, K, L, M, N, P) Al for 6 h and then harvested for further experiments. A and B, Scanning electron micrographs of the control and Al-treated cells. Bars, 5 μm. C to F, Transmission electron micrographs of control cells and Al-treated cells. Insets, Arrows point to regions of nuclei with marginalized chromatin. Bars, 0.5 μm. N, Nucleus; M, mitochondrion; V, vacuole. G and H, Nuclear fragmentation (black arrows) and DNA degradation (white arrows) shown by DAPI staining. I to N, TUNEL assay. Boxes marked K and L are magnified in M and N using a Zeiss LSM image examiner. Positive TUNEL signals were detected mainly in Al-induced aggregate cells. O and P, Analysis of DNA content by flow cytometry in PI-stained cells.

using the RACE technique. Alignment analysis showed that PpBI-1 is the closest to rice (*Oryza sativa*) OsBI-1 and second to barley (*Hordeum vulgare*) HvBI-1 (Fig. 5, A and B), supporting the accepted evolutionary classification that BI-1 has a separation between monocotyledonous and dicotyledonous species (Bolduc et al., 2003).

The three antiapoptotic proteins (Ced-9, Bcl-2, and PpBI-1) in transgenic cells were examined by western blot (data not shown). To assess whether antiapoptotic members can enhance Al tolerance in yeast, growth power (OD_{600} values) of these strains was assayed in liquid medium. As shown in Figure 1B, all three antiapoptotic members could block Al-caused growth inhibition, especially at 0.2 and 0.5 mM Al levels. Based on their growth curves, cells harboring *Bcl-2* displayed less Al tolerance than those harboring *Ced-9* or *PpBI-1* (data not shown). No significant difference was found in synthetic dextrose (SD)/Gal-Raf/His (inducible expression) with no Al or in SD/Glu/His (no expression) with 0.5 mM Al (Fig. 1C), indicating that alleviation of Al-caused growth inhibition resulted from the action

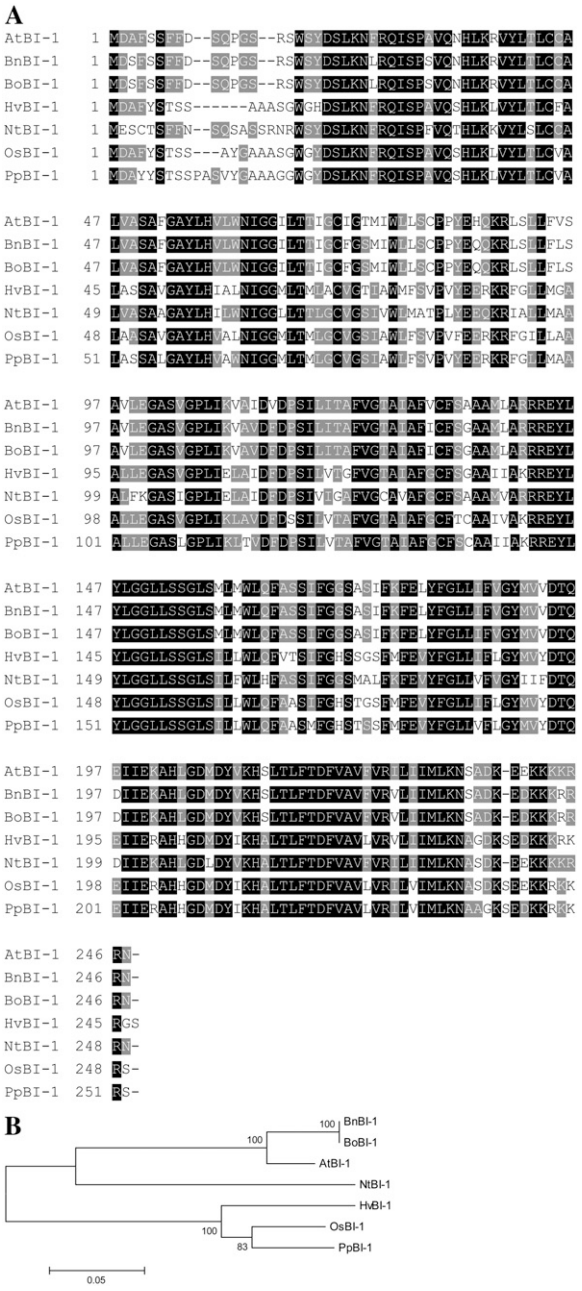

Figure 5. Sequence analysis of *BI-1* isolated from *P. praecox*. A, Multiple sequence alignment was generated by the AlignX program of Vector NTI Suite 6.0. Amino acids identical and conservative among these multiple sequences were shaded black and gray, respectively. B, Bootstrap test of phylogeny using Maga 2.1. Branch lengths are drawn to scale and numbers indicate frequencies of the same results presented out of 100 attempts using the bootstrap option of Maga 2.1. Accession numbers of plant *BI-1*s are as follows (in parentheses): *At*, Arabidopsis (AY091134); *Bn*, *Brassica napus* (AF390555); *Bo*, *Brassica oleracea* (AF453320); *Hv*, *H. vulgare* (AJ290421); *Nt*, *Nicotiana tabacum* (AF390556); *Os*, *O. sativa* (AB025926); *Pp*, *P. praecox* (DQ277647).

of antiapoptotic members. Also, the three members all enhanced the viability of Al-exposed cells (Fig. 3, B and D), which indirectly supported the idea that Al induces yeast cell death through the PCD pathway.

To further assess the function of antiapoptotic members, sensitivity tests between H_2O_2, heat shock, and Al were carried out (Fig. 6). First, at 30°C (normal temperature) without Al or H_2O_2, all four strains showed the same growth status after 3 d. Second, cells expressing Ced-9 and PpBI-1 exhibited almost equivalently increased tolerance to Al, heat shock, and H_2O_2 under all conditions tested. Interestingly, whether Al or H_2O_2 was added or not, Bcl-2 had far stronger growth ability at 37°C (a medium heat shock temperature) than at 30°C or 25°C. Additionally, cells expressing Ced-9, Bcl-2, and PpBI-1 could all survive better in 10 mM Al treatment than control cells after 10 d (data not shown). Together, our data show PCD-involved Al toxicity can be alleviated by antiapoptotic members (Ced-9, Bcl-2, and PpBI-1) in yeast, which may provide a novel mechanism for Al tolerance improvement.

Al-Elicited Elevation of Intracellular ROS

To determine whether Al toxicity elicited an intracellular ROS burst in its damage to yeast cells, flow cytometry was used to measure ROS-activated 2′,7′-dichlorohydrofluorescein diacetate (DCFH-DA) fluorescence. As shown in Figure 7, A and B, intracellular increased ROS levels depend on Al concentrations in yeast. Because high doses of Al with no DCFH-DA had little background fluorescence (data not shown), it is difficult to understand the continuously increased ROS levels at 54 mM Al regardless of enhanced cell viability (Fig. 3A). Although Al-stressed cells relative to nonstressed controls had elevated ROS levels for all cell types tested, Ced-9, Bcl-2, and PpBI-1 did not appear to significantly inhibit Al-elicited ROS production (Fig. 7, C–F), implying that these antiapoptotic members might not directly regulate Al-elicited ROS levels.

Al-Triggered Calcium Level Increase Blocked by Antiapoptotic Members

The above data have shown that three antiapoptotic members could significantly improve Al tolerance in yeast cells, but by which mechanism they execute their actions remains unclear. To further explore the functions of antiapoptotic members in Al tolerance, intracellular calcium-activated Fluo-3 fluorescence was measured using flow cytometry to monitor the change of intracellular Ca^{2+} signals. Whether 10 mM $CaCl_2$ was added or not, 6 mM Al treatment resulted in an increased Ca^{2+} level after 6 h (Fig. 8, A–D). Next, the dynamics of Al-triggered Ca^{2+} signals was monitored over time by recording fluorescent intensity. It is shown that Fluo-3-loaded cells exhibited transient magnification of Ca^{2+} signals when adding 6 mM Al to the

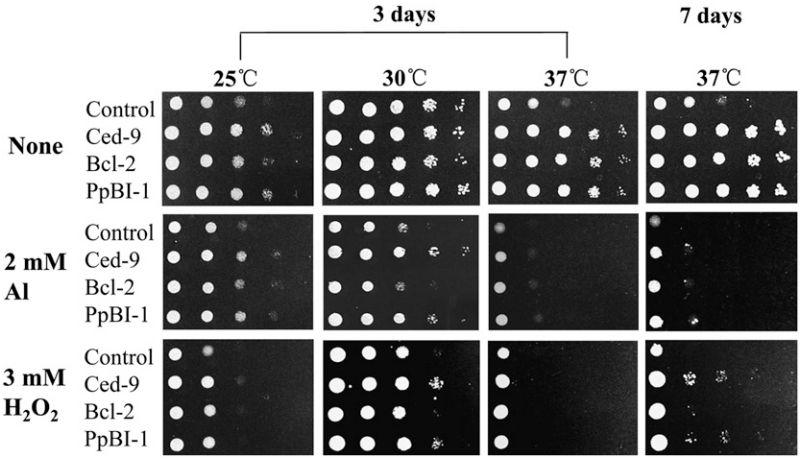

Figure 6. Sensitivity tests of cells expressing Ced-9, Bcl-2, and PpBI-1 challenged with Al, H_2O_2, and temperatures. Log-phase cells were diluted at 10-fold series with initial OD_{600} 2.5, and then 6 μL of each dilution were spotted on SD/Gal-Raf/His plates containing Al or H_2O_2 at indicated temperatures. Photos were taken after 3 or 7 d of incubation.

medium, and an exogenous Ca^{2+} application before or after Al treatment almost did not alter Ca^{2+} levels (Fig. 8, E and F). Furthermore, the Ca^{2+} signal levels detected in cells expressing Ced-9, Bcl-2, and PpBI-1 were distinctly less than those in control cells (Fig. 8, G–J), suggesting that antiapoptotic members act upstream of intracellular Ca^{2+} flux in the pathway to Al-induced PCD.

DISCUSSION

Al Promotes Cell Division in Yeast

In plant and animal cells, low concentrations of Al were reported to enhance cell division and growth (Morimura et al., 1978; Jones et al., 1986; Grauer and Horst, 1990; Kinraide, 1993; Yao et al., 1994; Clune and Coeland, 1999), but the mechanism of this effect is

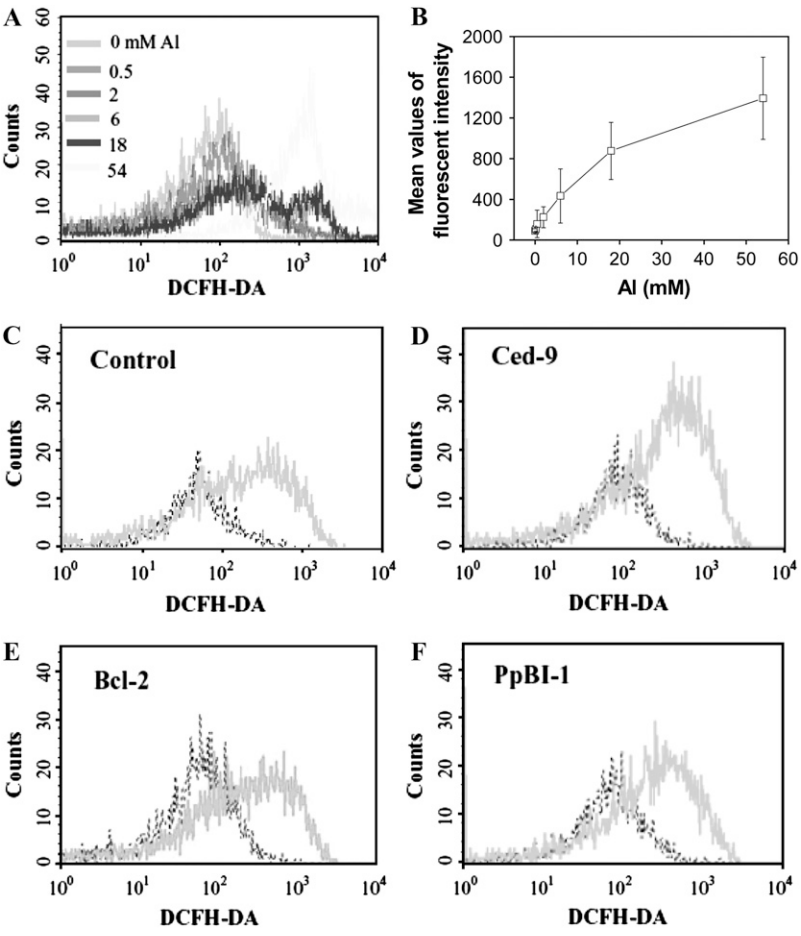

Figure 7. Al-elicited changes of intracellular ROS levels in yeast. A, Flow cytometric measurement for ROS changes of cells treated with various concentrations of Al for 6 h. B, Mean values of fluorescent intensity corresponding to A. C to F, ROS levels in yeast cells expressing Ced-9, Bcl-2, and PpBI-1, and the control cells harboring the empty vector after exposure to no Al (left shifted line) or 6 mM Al (right shifted line) for 6 h.

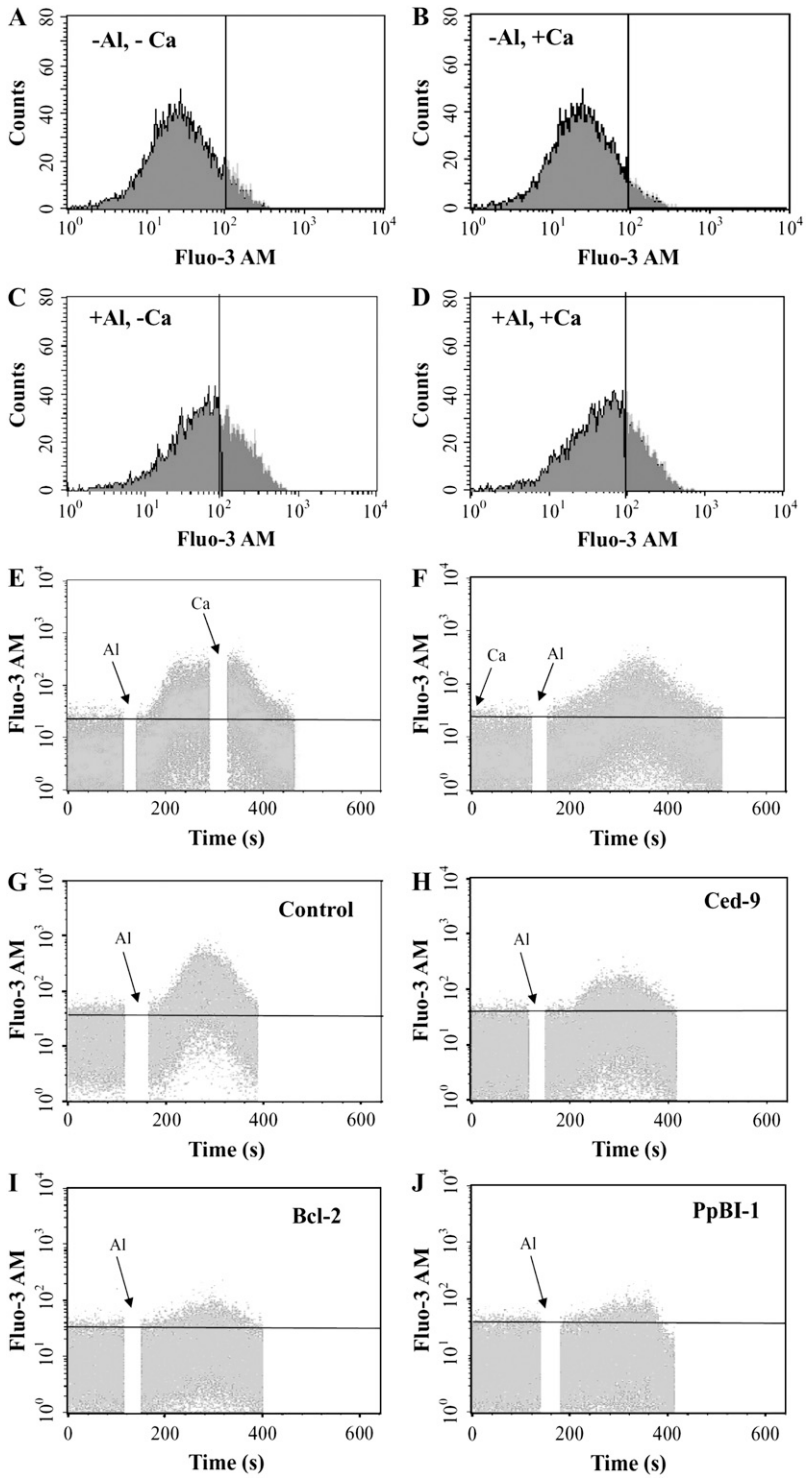

Figure 8. Al-triggered intracellular calcium elevation in yeast. A to D, Flow cytometric analysis of Al-challenged Ca^{2+} levels in control cells incubated in liquid medium for 6 h treated with 6 mM Al (+Al) or no (−Al) together with 10 mM $CaCl_2$ (+Ca) or no (−Ca). Exogenous Ca did not affect endogenous Ca^{2+} signals. A, Control without Al and exogenous Ca treatments. B, Control without Al treatment but supplemented with Ca. C, Al treatment unsupplemented with exogenous Ca. D, Al treatment supplemented with exogenous Ca. E and F, Dynamics of Al-triggered Ca^{2+} signals. Al and exogenous Ca concentrations are the same as in A to D. E, Exogenous Ca application after Al treatments. F, Al treatments after exogenous Ca application. G to J, Effects of the empty vector (G), Ced-9 (H), Bcl-2 (I), and PpBI-1 (J) on endogenous Ca^{2+} signals upon Al stress. Ced-9, Bcl-2, and PpBI-1 significantly blocked Al-elicited Ca^{2+} signals compared to the control.

uncertain, probably due to Al-influenced bioavailability of other metal ions stimulating cell growth. In this study, we found that Al promoted cell division in a dose- and cell density-dependent manner (Fig. 2). It is likely that there exists a dynamic balance between Al-promoted cell division and Al-caused cell death and their overlapped effect ultimately decides cell fate—growth or death. We suppose that Al at relatively low levels more actively participates in various physiological processes besides its toxicity to cells. Noticeably, in our study, Al levels promoting cell division are relatively high compared with those in the above-mentioned reports, probably resulting from different yeast media.

Antiapoptotic Members Attenuate Al-Induced PCD and Enhance Al Tolerance

Apoptosis occurs as a major type of PCD responding to various kinds of intrinsic and extrinsic stimuli. Upon Al stress, cell abnormal aggregation and DNA fragmentation have been found in neurons (Suárez-Fernández et al., 1999; Fu et al., 2003) and plant cells (Pan et al., 2001; Zhu et al., 2003), and Al directly binding to nuclear DNA probably occurs to change the structure of chromatin (Matsumoto, 1988). It has been indicated that Al causes irregular vacuolation in yeast cells (Ezaki et al., 1998). Our detailed observations show that cell shrinkage, vacuolation, chromatin marginalization, nuclear fragmentation and DNA degradation, DNA strand breaks, as well as abnormal cell aggregation occur during Al-induced cell death (Figs. 3 and 4), suggesting that Al induces PCD in yeast cells with important hallmarks of apoptosis.

In an attempt to test our hypothesis regarding whether blocking Al-induced PCD can alleviate Al toxicity and enhance tolerance in yeast cells, we assessed the roles of antiapoptotic members on Al toxicity. Our data show that antiapoptotic members are able to tolerate low-level Al-caused growth inhibition (Figs. 1 and 6) and suppress Al-caused cell death (Fig. 3). At high Al levels directly blocking cell growth, the function of these members is evaluated by their ability to delay Al-induced PCD. It was reported that Bcl-2 and Ced-9 could suppress H_2O_2-caused cell death in yeast, but verapamil (a chemical not associated with PCD) could not (Chen et al., 2003). Therefore, our data imply that the negative regulation of PCD provides a novel potential mechanism of Al tolerance, with important implications for genetic improvement of crops.

Interestingly, the survival-enhancing ability together with the growth-retarding effect of Bcl-2 in yeast lets us consider its well-known dual function in animals (Mazel et al., 1996; Bonnefoy-Berard et al., 2004). Sensitivity of proliferating cells to stimuli usually relies on the phase of the cell cycle and perhaps cells out of the stationary phase are more vulnerable to stresses in the environment. Actually, the importance of regulating the cell cycle under Al stress has been highlighted (Yamamoto et al., 1994; Schott and Gardner, 1997; Guo and Liang, 2001). Taking account of our results, we suppose the following. (1) When cells go on dividing at low levels of Al, Bcl-2 differs from Ced-9 and PpBI-1 in Al tolerance probably due to the dual function of Bcl-2; and (2) the PCD-inhibitory function of Bcl-2 can be clearly evaluated at high levels of Al because its dual function may not work when cell cycles are blocked.

Antiapoptotic Members Modulate Ca Flux But Not ROS Levels in Response to Al Stress

It is widely accepted that ROS are endogenous regulating signals of apoptosis (Costa and Moradas-Ferreira, 2001). Contradictorily, apoptosis can occur without ROS mediation (Fleury et al., 2002a). Based on the parallel results from the functional test of antiapoptotic members under Al and H_2O_2 stress, we address whether Al directly induces ROS production. One potential mechanism underlying Al-mediated cellular toxicity is the prooxidant action both in plants (Yamamoto et al., 2002; Boscolo et al., 2003) and animals (Murakami and Yoshino, 2004; Gómez et al., 2005). Although several reports in yeast implied a possible connection between Al toxicity and oxidative stress (Ezaki et al., 1998; Basu et al., 2004), there is no convincing evidence for Al-elicited ROS. In this study, intracellular ROS levels were directly measured using a cell-permeant oxidant-sensitive fluorescent probe, DCFH-DA. Our results showed a dose-dependent formation of intracellular ROS in response to added Al (Fig. 7, A and B). However, although ROS accumulated to higher levels at the highest Al concentration (54 mM), it is hard to explain why cell death did not increase in this case (Fig. 3A). In addition, the antiapoptotic members did not reduce ROS levels detectably despite protecting yeast cells from Al toxicity (Fig. 7, C–F). It is therefore likely that antiapoptotic members function downstream of ROS production or through ROS-independent pathways in response to Al stress.

The above results prompted us to explore Ca^{2+} signaling, which may sometimes occur following ROS production (Brookes et al., 2004). Intracellular Ca^{2+} takes dual responsibility not only for regulation of cell survival, but also for promotion of cell death in response to a variety of pathological conditions, which may depend on its concentration (Hajnóczky et al., 2003). In plants, Al toxicity was suggested to compromise intracellular Ca^{2+} homeostasis and block the Ca^{2+} influx channel on the plasma membrane (Huang et al., 1996; Jones et al., 1998; Ma et al., 2002; Kawano et al., 2004). In yeast, however, the relations between Al toxicity and Ca^{2+} signaling remain obscure. From our data herein, Al can transiently elicit a striking increase of intracellular free Ca^{2+} signals with later elevation at comparatively higher levels after long-time treatment (Fig. 8, A–F). Data from Ca^{2+}-free and Ca^{2+}-containing conditions imply that intracellular Ca^{2+} redistribution instead of extracellular Ca^{2+} influx may be involved in Al toxicity. The antiapoptotic members were shown to dramatically alter Al-elicited Ca^{2+} signals (Fig. 8, G–J), which might be a potential way by which they execute protective functions. Bcl-2 has been proved to maintain intracellular calcium homeostasis (Pinton et al., 2002; Chami et al., 2004), and some evidence has been presented for the supposition that BI-1 may serve as a pore or ion channel in the endoplasmic reticulum for calcium handling (Xu and Reed, 1998; Chae et al., 2004). It is worth mentioning that the major Ca^{2+} storage in yeast is the vacuole, distinguishing it from that in mammals (Cunningham and Fink, 1994). Therefore, clarifying the regulation process in Al-induced PCD in yeast will be able to give us new insight into the mechanisms of Al toxicity and tolerance in plants.

MATERIALS AND METHODS

Culture Medium, Yeast Growth, and Viability

Cells were grown in SD/Gal-Raf/His (inducible) or SD/Glu/His (uninducible) medium (CLONTECH) with additional 1% agar, pH 4.0. $AlCl_3$ stock solutions with concentrations of 0.1 and 1 M were prepared after filter sterilization and added to liquid medium at room temperature or to plates below 50°C. Cells were preincubated in appropriate medium two times each with OD_{600} up to about 0.5. For growth assays, the initial OD_{600} was adjusted to 0.05 (otherwise specified), and shaken at 200 rpm, 30°C. OD_{600} was measured by spectrophotometer and cell density was calculated using a standard hemocytometer. For spot assays, the OD_{600} of each cell culture was adjusted to 2.5, diluted at 10-fold series (1:1, 1:10, 1:100, 1:1,000, 1:10,000), and then aliquots (6 μL) of each dilution were spotted onto a SD/Gal-Raf/His plate with or without treatment before incubation at selected temperatures. Cell viability was evaluated by the plate count method. The cultured cells were harvested for certain intervals, diluted to the equal cell density with OD_{600} 0.0005, and then 30 μL of each cell sample were plated onto YPD (1% yeast extract, 2% Difco peptone, 2% Glc) plates.

Isolation of the *PpBI-1* Gene

Based on conserved regions of *BI-1* among rice (*Oryza sativa*), barley (*Hordeum vulgare*), tobacco (*Nicotiana tabacum*), oilseed rape (*Brassica napus*), and Arabidopsis (*Arabidopsis thaliana*) using the OMIGA program, some primers were designed (primer positions were indicated in the primer name based on *OsBI-1*). Total RNA was isolated from the flowers of *Phyllostachys praecox* and then transcribed to cDNA with BD PowerScript reverse transcriptase (CLONTECH). 5′- and 3′-RACE-ready cDNA were synthesized, respectively, according to the BD SMARTRACE cDNA amplification kit user manual (BD Biosciences CLONTECH). Then 5′- and 3′-end fragments of *PpBI-1* were amplified, respectively: 3′-end fragment primers, *BI-1*(72–97)-P1 (5′-GAACTTCCGCCAGATCTCCCCCGCCG-3′), L (5′-CTAATACGACTCACTATAGGGCAAGCAGTGGTATCAACGCAGAGT-3′), and S (5′-CTAATACGACTCACTATAGGGC-3′); and 5′-end fragment primers, *BI-1*(480–456)-P2 (5′-CAGGATCGAGAGGCCAGAAGAGAGC-3′), L, and S. Additionally, a nest primer *BI-1*(365–342)-P2 (5′-GTCACGAGAATGCTTGGGTCAAAG-3′) was also used to amplify the 5′-end fragment. To obtain the real entire coding region of *PpBI-1*, primers *PpBI-1*-P1 (5′-CGAACTCGAGCCGATTCGATCCGGCTCACGCGAG-3′) with *Xho*I and *PpBI-1*-P2 (5′-CAACACTAGTGCCGTAGCAGCAGTAGACCCGGCC-3′) with *Spe*I were designed based on obtained sequences of 3′-and 5′-end fragments. Finally, an 843-bp PCR fragment was obtained with pfu polymerase and then cloned into the pBluescript SK+ vector. The open reading frame of *PpBI-1* was confirmed by sequencing and aligned with some reported *BI-1*s from other plant species.

Constructs and Transformation

Ced-9 (generously provided by R. Horvitz, Massachusetts Institute of Technology), *Bcl-2* (generously provided by S. Korsmeyer, Dana-Farber Cancer Institute), and *PpBI-1* (in our lab) were digested with *Eco*RI and *Xho*I, and then cloned into the yeast-inducible expression vector pGilda (generously provided by P.H. Ho, the Burnham Institute), which harbors a CEN/ARS replication origin, a GAL1 promoter, and a His selection marker (Kampranis et al., 2000), resulting in pGilda-*Ced-9*, pGilda-*Bcl-2*, and pGilda-*PpBI-1*, respectively. Sequencing further confirmed that the open reading frames of target genes were in frame with the LexA fusion part of pGilda. The three constructs (pGilda-*Ced-9*, pGild-*Bcl-2*, and pGilda-*PpBI-1*), together with the empty vector (pGilda), were respectively transformed into the budding yeast EGY48 (MATa, ura3, his3, trp1, 6LexA-operator-LEU2; generously provided by H.P. Chen, Fudan University; Chen et al., 2003), using the lithium acetate (LiAc) method. Positive transformants were identified by PCR and antiapoptotic proteins were assayed using anti-LexA antibody (Invitrogen) by western blot (Moon et al., 2002).

Microscopic Observation

For scanning electron microscopy, yeast cells were fixed with 2.5% glutaraldehyde, washed three times with 0.1 M phosphate-buffered saline (PBS), and spun down each time for 15 s and resuspended in 1% osmium tetroxide (OsO_4). Then the cells were dried in a critical point drier, gold sputter coated, and observed under a scanning electron microscope (Sambridge S260). For transmission electron microscopy, yeast cells were fixed with 2.5% glutaraldehyde, successively dehydrated with gradient ethanol series (50%, 70%, 90%) for 15 min, 100% ethanol for 20 min, 100% acetone two times for 20 min, and then infiltrated with acetone and Epon in a 1:1 mixture for 2 h and with 100% Epon for 20 h. Cells were then transferred to fresh 100% Epon and incubated at 56°C for 48 h. Ultrathin sections were stained with 4% uranium acetate for 20 min and plumbic citrate for 5 min, and intracellular ultrastructures were visualized under a transmission electron microscopy (Philips Em 410).

To detect nuclear fragmentation, yeast cells were fixed in 70% ethanol for at least 2 h and then washed with PBS, pH 7.4, and incubated with 1 μg/mL DAPI in PBS for 10 min in the dark at room temperature. To examine cell viability, cells were stained with both 5 μg/mL PI (0.5 mg/mL stock solution, dissolved in 50 mM sodium citrate) and 10 μg/mL FDA (1 mg/mL stock solution, dissolved in acetone) for 20 min in the dark at room temperature. To visualize DNA strand breaks, cells were fixed in 4% formaldehyde in PBS, pH 7.4, then treated with lyticase (Sigma) and stained with fluorescein isothiocyanate-labeled TUNEL reagent (in situ cell death detection kit; Roche Molecular Biochemicals; Madeo et al., 1999). DAPI fluorescence was excited by UV radiation (U) and filtered at 420 nm, and FDA-PI fluorescence was excited by visible radiation (V) and filtered at 515 nm, respectively. Photos were taken under a fluorescence microscope (Olympus VANOX-AH-1). TUNEL fluorescence was examined at a 488-nm excitation wavelength under a confocal laser-scanning microscope (LSM 510; Zeiss).

Flow Cytometric Studies

Yeast cells were grown in SD/Gal-Raf/His medium with or without treatment. After harvest, cells were resuspended in PBS, pH 7.4, and vortexed briefly for further experiments. For PI permeability assays, cells were directly stained with 5 μg/mL PI and incubated in the dark for 30 min at room temperature. Intracellular ROS production was measured by staining with DCFH-DA (Sigma) at a final concentration of 50 μM for 20 min (Chen et al., 2003). To measure DNA content (Guo and Liang, 2001), cells were fixed by 70% ethanol, resuspended in 1 mL of DNA staining solution (200 μg PI plus 2 mg RNase A added in 10 mL of PBS), and then incubated for 30 min at room temperature in the dark. For determination of intracellular Ca^{2+} levels (Scoltock et al., 2000), yeast cells were incubated in PBS, pH 7.4, at 37°C for 30 min with 5 μM Fluo-3-acetoxymethyl ester (Fluo-3/AM; Biotium) prepared with a 1 mM stock solution in dimethyl sulfoxide. A noncytotoxic detergent, pluronic F-127 (0.1%), was added to increase solubility of Fluo-3/AM. When the time course of intracellular Ca^{2+} kinetics was analyzed (Monteiro et al., 1999), 6 mM $AlCl_3$ and/or 10 mM $CaCl_2$ were added to cell-resuspending medium, pH 4.0, after loading with Fluo-3/AM. PI fluorescence was measured by FACSCalibur with 488-nm (blue) argon (Becton-Dickinson) in the FL2 channel and dichlorofluorescein and Fluo-3 fluorescence in the FL1 channel. Data acquisition was performed using CellQuest (3.1f) software and data analysis with ModFit LT (3.0) software (Variety Software House). Two thousand to 10,000 cells were measured for each analysis.

Statistical Analysis

Data were calculated as the mean of results from at least three independent experiments or one representative result of parallel experiments. The Origin 6.1 program was used for calculation. Error bars represent SD.

ACKNOWLEDGMENTS

The authors sincerely thank R. Horvitz (Massachusetts Institute of Technology, Cambridge), S. Korsmeyer (Dana-Farber Cancer Institute, Boston), J.C. Reed (the Burnham Institute, La Jolla, CA), M. Kawai-Yamada (Institute of Molecular and Cellular Biosciences, University of Tokyo), D.J. Yun (Biotechnology Research Center, Gyeongsang National University, Korea), P.H. Ho and G.S. Feng (the Burnham Institute, La Jolla, CA), and H.P. Chen (Fudan University, China) for gifts of either plasmids or strains. We also thank H.M. Chen and Z.Y. Fang (College of Life Sciences, Zhejiang University, China), Z.M. Jiang (Zhejiang Tumor Hospital, China), and Y.J. Wang (Merck Research Laboratories, West Point, PA) for kind help. We are grateful to H. Matsumoto (Research Institute for Bioresources, Okayama University, Japan) for critical reading of the manuscript.

Received April 23, 2006; accepted July 10, 2006; published July 21, 2006.

LITERATURE CITED

Anoop VM, Basu U, McCammon MT, McAlister-Henn L, Taylor GJ (2003) Modulation of citrate metabolism alters aluminum tolerance in yeast and transgenic canola overexpressing a mitochondrial citrate synthase. Plant Physiol **132:** 2205–2217

Aremu DA, Meshitsuka S (2005) Accumulation of aluminum by primary cultured astrocytes from aluminum amino acid complex and its apoptotic effect. Brain Res **1031:** 284–296

Basu U, Southron JL, Stephens JL, Taylor GJ (2004) Reverse genetic analysis of the glutathione metabolic pathway suggests a novel role of *PHGPX* and *URE2* genes in aluminum resistance in *Saccharomyces cerevisiae*. Mol Genet Genomics **271:** 627–637

Bolduc N, Ouellet M, Pitre F, Brisson LF (2003) Molecular characterization of two plant BI-1 homologues which suppress Bax-induced apoptosis in human 293 cells. Planta **216:** 377–386

Bonnefoy-Berard N, Aouacheria A, Verschelde C, Quemeneur L, Marcais A, Marvel J (2004) Control of proliferation by Bcl-2 family members. Biochim Biophys Acta **1644:** 159–168

Boscolo PRS, Menossi M, Jorge RA (2003) Aluminum-induced oxidative stress in maize. Phytochemistry **62:** 181–189

Brookes PS, Yoon Y, Robotham JL, Anders MW, Sheu SS (2004) Calcium, ATP, and ROS: a mitochondrial love-hate triangle. Am J Physiol Cell Physiol **287:** 817–833

Chae HJ, Ke N, Kim HR, Chen SR, Godzik A, Dickman M, Reed JC (2003) Evolutionarily conserved cytoprotection provided by Bax Inhibitor-1 homologs from animals, plants, and yeast. Gene **323:** 101–113

Chae HJ, Kim HR, Xu CY, Bailly-Maitre B, Krajewska M, Krajewski S, Banares S, Cui J, Digicaylioglu M, Ke N, et al (2004) BI-1 regulates an apoptosis pathway linked to endoplasmic reticulum stress. Mol Cell **15:** 355–366

Chami M, Prandini A, Campanella M, Pinton P, Szabadkai G, Reed JC, Rizzuto R (2004) Bcl-2 and Bax exert opposing effects on Ca^{2+} signaling, which do not depend on their putative pore-forming region. J Biol Chem **279:** 54581–54589

Chen SR, Dunigan DD, Dickman MB (2003) Bcl-2 family members inhibit oxidative stress-induced programmed cell death in *Saccharomyces cerevisiae*. Free Radic Biol Med **34:** 1315–1325

Clune TS, Coeland L (1999) Effects of aluminum on canola roots. Plant Soil **216:** 27–33

Costa V, Moradas-Ferreira P (2001) Oxygen stress and signal transduction in *Saccharomyces cerevisiae*: insights into ageing, apoptosis and diseases. Mol Aspects Med **22:** 217–246

Cunningham KW, Fink GR (1994) Ca^{2+} transport in *Saccharomyces cerevisiae*. J Exp Biol **196:** 157–166

Delhaize E, Ryan PR, Hebb DM, Yamamoto Y, Sasaki T, Matsumoto H (2004) Engineering high-level aluminum tolerance in barley with the ALMT1 gene. Proc Natl Acad Sci USA **42:** 15249–15254

Devi SR, Yamamoto Y, Matsumoto H (2003) An intracellular mechanism of aluminum tolerance associated with high antioxidant status in cultured tobacco cells. J Inorg Biochem **97:** 59–68

Dickman MB, Park YK, Oltersdorf T, Li W, Clemente T, French R (2001) Abrogation of disease development in plants expressing animal antiapoptotic genes. Proc Natl Acad Sci USA **98:** 6957–6962

Dion M, Chamberland H, St-Michel C, Plante M, Darveau A, Lafontaine JG, Brisson LF (1997) Detection of a homologue of bcl-2 in plant cells. Biochem Cell Biol **75:** 457–461

Eichmann R, Schultheiss H, Kogel KH, Hückelhoven R (2004) The barley apoptosis suppressor homologue Bax inhibitor-1 compromises nonhost penetration resistance of barley to the inappropriate pathogen *Blumeria graminis* f. sp. *tritici*. Mol Plant Microbe Interact **17:** 484–490

Ezaki B, Gardner RC, Ezaki Y, Kondo H, Matsumoto H (1998) Protective roles of two aluminum (Al)-induced genes, *HSP150* and *SED1* of *Saccharomyces cerevisiae* in Al and oxidative stresses. FEMS Microbiol Lett **159:** 99–105

Ezaki B, Gardner RC, Ezaki Y, Matsumoto H (2000) Expression of aluminum-induced genes in transgenic Arabidopsis plants can ameliorate aluminum stress and/or oxidative stress. Plant Physiol **122:** 657–665

Ezaki B, Katsuhara M, Kawamura M, Matsumoto H (2001) Different mechanisms of four aluminum (Al)-resistant transgenes for Al toxicity in Arabidopsis. Plant Physiol **127:** 918–927

Ezaki B, Sivaguru M, Ezaki Y, Matsumoto H, Gardner RC (1999) Acquisition of aluminum tolerance in *Saccharomyces cerevisiae* by expression of the *BCB* or *NtGDI1* gene derived from plants. FEMS Microbiol Lett **171:** 81–87

Fleury C, Mignotte B, Vayssière JL (2002a) Mitochondrial reactive oxygen species in cell death signaling. Biochimie **84:** 131–141

Fleury C, Pampin M, Tarze A, Mignotte B (2002b) Yeast as a model to study apoptosis? Biosci Rep **22:** 59–79

Fu HJ, Hu QS, Lin ZN, Ren TL, Song H, Cai CK, Dong SZ (2003) Aluminum-induced apoptosis in cultured cortical neurons and its effect on SAPK/JNK signal transduction pathway. Brain Res **980:** 11–23

Gómez M, Esparza JL, Nogués MR, Giralt M, Cabré M, Domingo JL (2005) Pro-oxidant activity of aluminum in the rat hippocampus: gene expression of antioxidant enzymes after melatonin administration. Free Radic Biol Med **38:** 104–111

Grauer UE, Horst WJ (1990) Effect of pH and nitrogen source on aluminum tolerance of rye (*Secale cereale* L.) and yellow lupin (*Lupinus luteus* L.). Plant Soil **127:** 13–21

Guo GW, Liang YX (2001) Aluminum-induced apoptosis in cultured astrocytes and its effect on calcium homeostasis. Brain Res **888:** 221–226

Hajnóczky G, Davies E, Madesh M (2003) Calcium signaling and apoptosis. Biochem Biophys Res Commun **304:** 445–454

Huang JW, Pellet DM, Papernik LA, Kochian LV (1996) Aluminum interactions with voltage-dependent calcium transport in plasma membrane vesicles isolated from roots of aluminum-sensitive and -resistant wheat cultivars. Plant Physiol **110:** 561–569

Hückelhoven R (2004) BAX Inhibitor-1, an ancient cell death suppressor in animals and plants with prokaryotic relatives. Apoptosis **9:** 299–307

Jin C, Reed JC (2002) Yeast and apoptosis. Nat Mol Cell Biol **3:** 453–459

Jones DL, Kochian LV, Gilroy S (1998) Aluminum induces a decrease in cytosolic calcium concentration in BY-2 tobacco cell cultures. Plant Physiol **116:** 81–89

Jones TR, Antonetti DL, Reid TW (1986) Aluminum ions stimulate mitosis in murine cells in tissue culture. J Cell Biochem **30:** 31–39

Kampranis SC, Damianova R, Atallah M, Toby G, Kondi G, Tsichlis PN, Makris AM (2000) A novel plant glutathione S-transferase/peroxidase suppresses Bax lethality in yeast. J Biol Chem **275:** 29207–29216

Kawai-Yamada M, Jin L, Yoshinaga K, Hirata A, Uchimiya H (2001) Mammalian Bax-induced plant cell death can be down-regulated by overexpression of *Arabidopsis Bax Inhibitor-1* (AtBI-1). Proc Natl Acad Sci USA **98:** 12295–12300

Kawai-Yamada M, Ohori Y, Uchimiya H (2004) Dissection of Arabidopsis Bax inhibitor-1 suppressing Bax-, hydrogen peroxide-, and salicylic acid-induced cell death. Plant Cell **16:** 21–32

Kawano T, Kadono T, Fumoto K, Lapeyrie F, Kuse M, Isobe M, Furuichi T, Muto S (2004) Aluminum as a specific inhibitor of plant TPC1 Ca^{2+} channels. Biochem Biophys Res Commun **324:** 40–45

Kinraide TB (1993) Aluminum enhancement of plant growth in acid rooting media. A case of reciprocal alleviation of toxicity by two toxic cations. Physiol Plant **88:** 619–625

Kochian LV, Hoekenga OA, Piñeros MA (2004) How do crop plants tolerate acid soils? Mechanisms of aluminum tolerance and phosphorous efficiency. Annu Rev Plant Biol **55:** 459–493

Lawen A (2003) Apoptosis—an introduction. Bioessays **25:** 888–896

LeBrasseur N (2004) Yeast apoptosis debate continues. J Cell Biol **166:** 938

Ma Q, Rengel Z, Kuo J (2002) Aluminum toxicity in rye (*Secale cereale*): root growth and dynamics of cytoplasmic Ca^{2+} in intact root tips. Ann Bot (Lond) **89:** 241–244

MacDiarmid CW, Cardner RC (1996) Al toxicity in yeast. Plant Physiol **112:** 1101–1109

MacDiarmid CW, Gardner RC (1998) Overexpression of the *Saccharomyces cerevisiae* magnesium transport system confers resistance to aluminum ion. J Biol Chem **273:** 1727–1732

Madeo F, Fröhlich E, Ligr M, Grey M, Sigrist SJ, Wolf DH, Fröhlich KU (1999) Oxygen stress: a regulator of apoptosis in yeast. J Cell Biol **145:** 757–767

Madeo F, Herker E, Wissing S, Jungwirth H, Eisenberg T, Fröhlich KU (2004) Apoptosis in yeast. Curr Opin Microbiol **7:** 655–660

Matsumoto H (1988) Changes of the structure of pea chromatin by aluminum. Plant Cell Physiol **29:** 281–287

Matsumoto H (2000) Cell biology of aluminum toxicity and tolerance in higher plants. Int Rev Cytol **200:** 1–46

Matsumura H, Nirasawa S, Kiba A, Urasaki N, Saitoh H, Ito M, Kawai-Yamada M, Uchimiya H, Terauchi R (2003) Overexpression of Bax inhibitor suppresses the fungal elicitor-induced cell death in rice (Oryza sativa L.) cells. Plant J **33:** 425–434

Mazel S, Burtrum D, Petrie HT (1996) Regulation of cell division cycle progression by *bcl-2* expression: a potential mechanism for inhibition of programmed cell death. J Exp Med **183:** 2219–2226

Mitsuhara I, Malik KA, Miura M, Ohashi Y (1999) Animal cell-death suppressors Bcl-X_L and Ced-9 inhibit cell death in tobacco plants. Curr Biol **9:** 775–778

Monteiro MC, Sansonetty F, Gonçalves MJ, O'Connor J (1999) Flow cytometric kinetic assay of calcium mobilization in whole blood platelets using Fluo-3 and CD41. Cytometry **35:** 302–310

Moon H, Baek D, Lee B, Prasad DT, Lee SY, Cho MJ, Lim CO, Choi MS, Bahk J, Kim MO, et al (2002) Soybean ascorbate peroxidase suppresses Bax-induced apoptosis in yeast by inhibiting oxygen radical generation. Biochem Biophys Res Commun **290:** 457–462

Morimura S, Takakahashi E, Matsumoto H (1978) Association of aluminum with nuclei and inhibition of cell division in onion (Allium cepa) roots. Z Pflanzenphysiol **88:** 395–401

Murakami K, Yoshino M (2004) Aluminum decreases the glutathione regeneration by the inhibition of NADP-isocitrate dehydrogenase in mitochondria. J Cell Biochem **93:** 1267–1271

Pan JW, Zheng K, Ye D, Yi HL, Jiang ZM, Jing CT, Pan WH, Zhu MY (2004) Aluminum-induced ultraweak luminescence changes and sister-chromatid exchanges in root tip cells of barley. Plant Sci **167:** 1391–1399

Pan JW, Zhu MY, Chen H (2001) Aluminum-induced cell death in root-tip cells of barley. Environ Exp Bot **46:** 71–79

Pinton P, Ferrari D, Rapizzi E, Virgilio FD, Pozzan T, Rizzuto R (2002) A role for calcium in Bcl-2 action? Biochimie **84:** 195–201

Sasaki T, Yamamoto Y, Ezaki B, Katsuhara M, Ahn SJ, Ryan PR, Delhaize E, Matsumoto H (2004) A wheat gene encoding Al-activated malate transporter. Plant J **37:** 645–653

Savory J, Herman MM, Ghribi O (2003) Intracellular mechanisms underlying aluminum-induced apoptosis in rabbit brain. J Inorg Biochem **97:** 151–154

Schott EJ, Gardner RC (1997) Aluminum-sensitive mutants of *Saccharomyces cerevisiae.* Mol Gen Genet **254:** 63–72

Scoltock AB, Bortner CD, Bird GSJ, Putney JW, Cidlowski JA (2000) A selective requirement for elevated calcium in DNA degradation, but not early events in anti-Fas-induced apoptosis. J Biol Chem **275:** 30586–30596

Suárez-Fernández MB, Soldado AB, Sanz-Medel A, Vega JA, Novelli A, Fernández-Sánchez MT (1999) Aluminum-induced degeneration of astrocytes occurs via apoptosis and results in neuronal death. Brain Res **835:** 125–136

Watanabe N, Lam E (2006) Arabidopsis Bax inhibitor-1 functions as an attenuator of biotic and abiotic types of cell death. Plant J **45:** 884–894

Xu P, Rogers SJ, Roossinck MJ (2004) Expression of antiapoptotic genes *bcl-xL* and *ced-9* in tomato enhances tolerance to viral-induced necrosis and abiotic stress. Proc Natl Acad Sci USA **101:** 15805–15810

Xu QL, Reed JC (1998) Bax Inhibitor-1, a mammalian apoptosis suppressor identified by functional screening in yeast. Mol Cell **1:** 337–346

Yamaguchi Y, Yamamoto Y, Matsumoto H (1999) Cell death process initiated by a combination of aluminum and iron in suspension-cultured tobacco cells (*Nicotiana tobacum*): apoptosis-like cell death mediated by calcium and proteinase. Soil Sci Plant Nutr **45:** 647–657

Yamamoto Y, Kobayashi Y, Devi SR, Rikiishi S, Matsumoto H (2002) Aluminum toxicity is associated with mitochondrial dysfunction and the production of reactive oxygen species in plant cells. Plant Physiol **128:** 63–72

Yamamoto Y, Rikiishi S, Chang YC, Ono K, Kasai M, Matsumoto H (1994) Quantitative estimation of aluminum toxicity in cultured tobacco cells: correlation between aluminum uptake and growth inhibition. Plant Cell Physiol **35:** 575–583

Yao X, Jenkins EC, Wisniewski HM (1994) Effect of aluminum chloride on mitogenesis, mitosis, and cell cycle in human short-term whole blood cultures: lower concentrations enhance mitosis. J Cell Biochem **54:** 473–477

Zhu MY, Ahn SJ, Matsumoto H (2003) Inhibition of growth and development of root border cells by Al. Physiol Plant **117:** 359–367